

Unambiguous assignment of ^{13}C NMR signals in epimeric 4,5-epoxy-3-oxo-steroids assisted by X-ray diffraction and gauge invariant atomic orbitals calculation of absolute isotropic shieldings

Pablo Labra-Vázquez,^a Annia Galano,^b Margarita Romero-Ávila,^a
Marcos Flores-Álamo^a and Martín A. Iglesias-Arteaga^{a*}

^a *Facultad de Química, Universidad Nacional Autónoma de México,
Ciudad Universitaria, 04510 México, D.F., México*

^b *Departamento de Química, División de Ciencias Básicas e Ingeniería, Universidad Autónoma
Metropolitana Iztapalapa, 09340 México D.F., México*

E-mail: martin.iglesias@unam.mx

Abstract

Complete assignments of the ^{13}C signals of diastereomeric 4,5-epoxy-3-oxo steroids based on a combination of 1D and 2D NMR techniques are described. The assignments were corroborated or corrected by calculation of the absolute isotropic ^{13}C NMR shieldings using the Gauge Invariant Atomic Orbitals (GIAO) method at B3LYP/6-31+G(d,p) level.

Keywords: 4,5-Epoxy-3-oxo-steroids, NMR, Absolute isotropic ^{13}C NMR shielding calculations, X-ray structure

Introduction

Steroids play different roles in living organisms from both animal and vegetal kingdoms. In a wide variety of steroids, the coexistence of different functionality in the steroidal nucleus confers several properties that are interesting from both the biological and the synthetic points of view. In particular, steroids containing the 4,5-epoxy-3-oxo moiety are of special utility as synthetic precursors of a wide variety of polyfunctional derivatives or rearranged compounds.¹⁻⁵

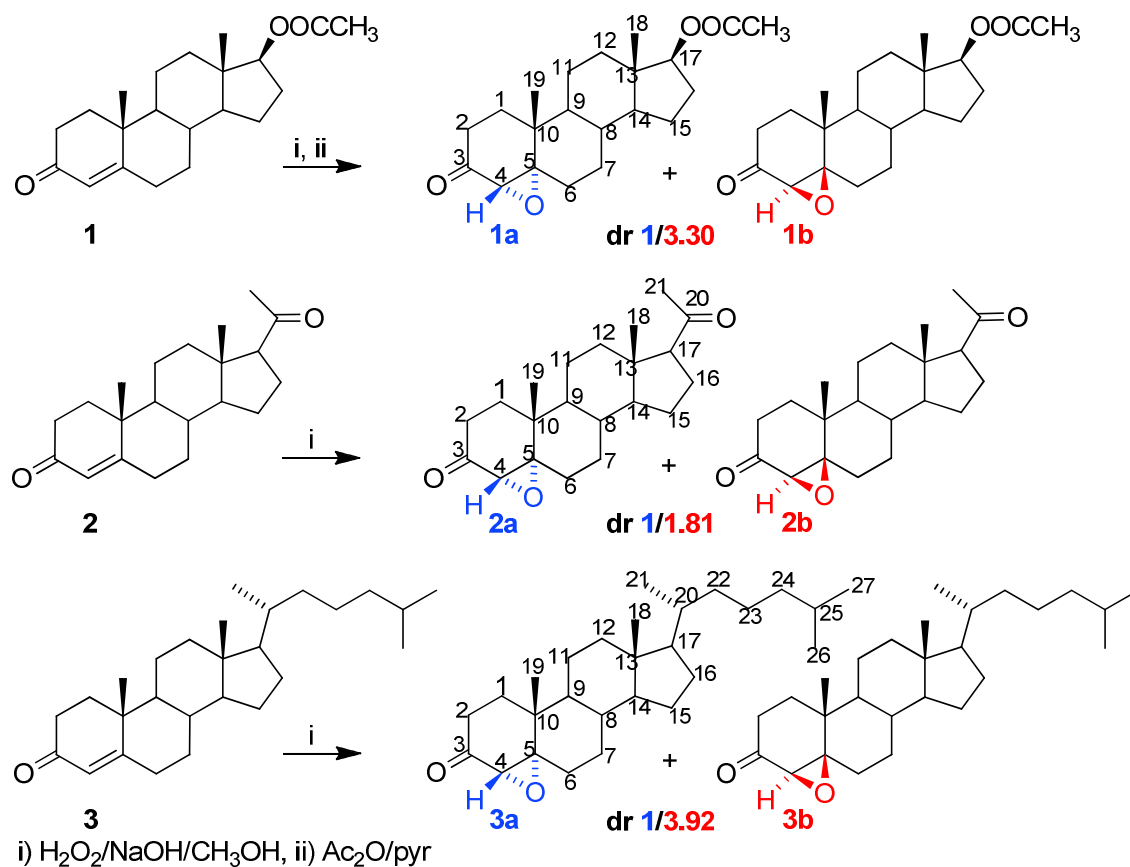
4,5-Epoxy-3-oxo-steroids can be prepared in moderate to good yield and varying diastereoselectivity by treatment with different reagents that include peracids,⁴ H_2O_2 in alkaline media,⁵ dioxiranes⁶ and more recently magnesium bis(monoperoxyphthalate) hexahydrate.⁷ In spite that such compounds have been extensively employed as synthetic precursors for different polyfunctional or rearranged steroids, no complete and unambiguous assignment of the ^{13}C NMR signals of such compounds is available. This may obey to the fact that in most of the synthetic

applications, 4,5-epoxy-3-oxo-steroids have been employed as diastereomeric mixtures, regardless that the different reactivity profile of each diastereomer may affect (or not) the yield.

As a part of our ongoing program on the synthesis of potentially bioactive steroids,⁸⁻¹¹ we require the unambiguous NMR characterization several pairs of epimeric epoxides derived from different 4-en-3-oxo-steroids that are being employed as synthetic precursors. Herein we report on the unambiguous ¹³C NMR assignments of series of epimeric 4,5-epoxy-3-oxo-steroids, assisted by X-ray diffraction and Gauge Invariant Atomic Orbitals Calculation of Absolute Isotropic Shieldings.

Results and Discussion

Treatment of methanol solutions of the 4-en-3-oxo-steroids **1-3** with H₂O₂ and NaOH produced mixtures of the corresponding α and β -epoxides. In the case of testosterone acetate (**1**) the epoxidation was accompanied with the partial saponification of the acetate at C-17 that was re-acetylated by treatment with acetic anhydride in pyridine (see Scheme 1). The diastereomeric relation in each epoxide pair was calculated by relative integration of the ¹H NMR signals corresponding to H-4 in the crude mixtures.



Scheme 1. Epoxidation of 4-en-3-oxo-steroids.

^1H NMR Analysis and structure determination

At first glance the β -orientation of H-4 in a $4\alpha,5$ -epoxy-steroid suggests that observation of a H-19 \leftrightarrow H-4 NOE effect should provide evidence enough to differentiate the α -epoxide from its β -epimer in which such effect should be not observed due to the α -orientation of H-4.

The NOESY experiment ran with the epoxide **1a** showed no conclusive NOE correlation between the H-4 signal at 3.02 ppm and the signal corresponding to the 19-methyl group at 1.05 ppm. This experiment showed a cross peak between the signal of H-4 ppm with a proton that resonates at 1.11 ppm that was identified as the equatorial H-6 α . Unfortunately this NOE correlation provides no evidence on the orientation of the oxirane ring because it is possible in both the α and β -epoxides.

Determination of the orientation of the oxirane ring in epoxide **1b** by observation of H-19 \leftrightarrow H-4 NOE effect is also hindered by overlapping of the appropriate ^1H signals. The NOESY experiment ran with the epoxide **1b** showed a weak cross peak between the signals at 2.96 ppm (H-4) and 1.14 ppm (*circa* resonance of H-19) that may lead to assume the β -orientation of H-4, and consequently to the wrong (*vide infra*) assignation of the α -orientation to the oxirane ring in epoxide **1b**. Carefully examination of HSQC correlations evidenced that the signal corresponding to at least one of the protons attached to C-6 appears between 1.14 and 1.13 ppm overlapping the signal of H-19. This results in the unsolvable disjunctive to assume that the mentioned cross peak is due to a H-4 \leftrightarrow H-19 NOE effect that would lead to the mistaken assignment of the α -orientation to epoxide **1b** (*vide infra*) or attribute the mentioned cross peak to a H-4 \leftrightarrow H-6 α NOE effect, that is possible in both, the α - and β -epoxides.

After failure of the determination of the orientation of the orientation of the oxirane rings in compounds **1a** and **1b** by NOESY, our attention was focused in obtaining crystals of each compound suitable for crystallographic studies. Slow evaporation of ethyl acetate solutions of epoxides **1a** and **1b** afforded monocrystals that allowed the truthful determination of the respective α and β -orientation of the oxirane rings in epoxides **1a** and **1b**. Figure 1 shows the crystal structures of epoxides **1a** and **1b** with the thermal ellipsoids drawn at 50% of probability.

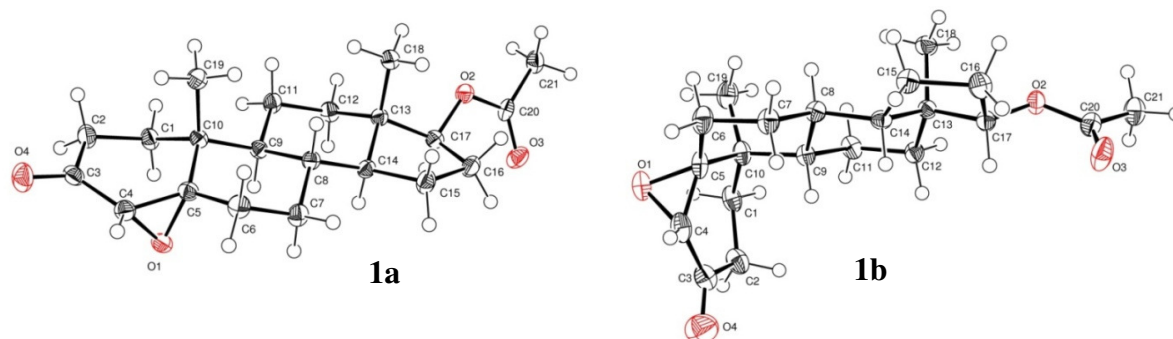
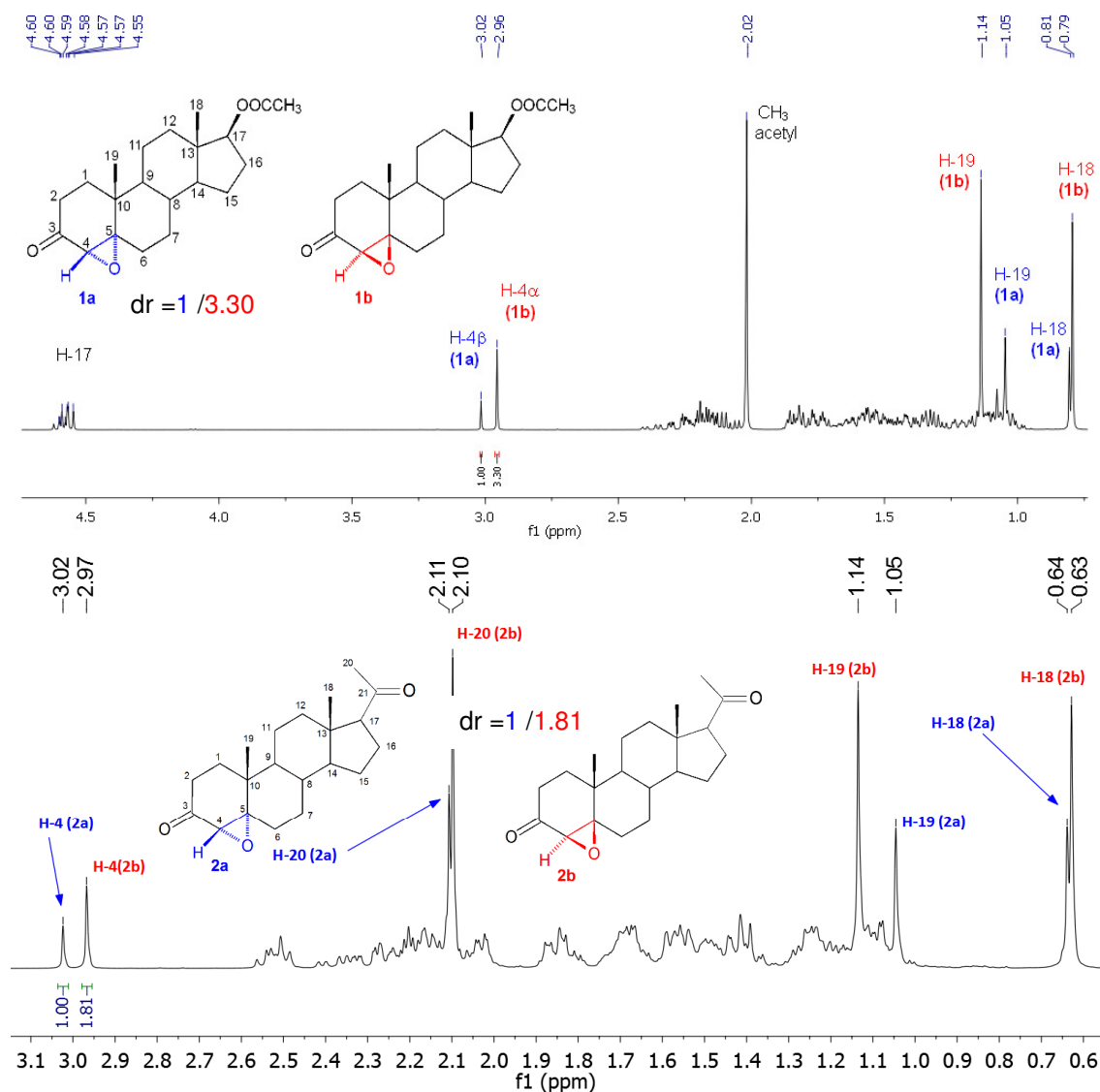


Figure 1. ORTEP drawings of the epoxides **1a** and **1b**.

Accordingly, the ^1H NMR spectra of the α -epoxide **1a** and its β -partner **1b** are characterized by the presence of the signals H-4 that appear at 3.02 and 2.96 ppm respectively. The signals of H-19, that appear at 1.05 ppm for the α -epoxide **1a** and at 1.14 ppm for the β -epimer, also characterize the spectra of the epoxidated compounds. These criteria, that was extended to the diastereomeric pairs **2a/b** and **3a/b**, can be generalized for the fast differentiation and quantification of each component in diastereomeric mixtures of 4,5-epoxy-3-oxo steroids (see Table 1 and Figure 2).



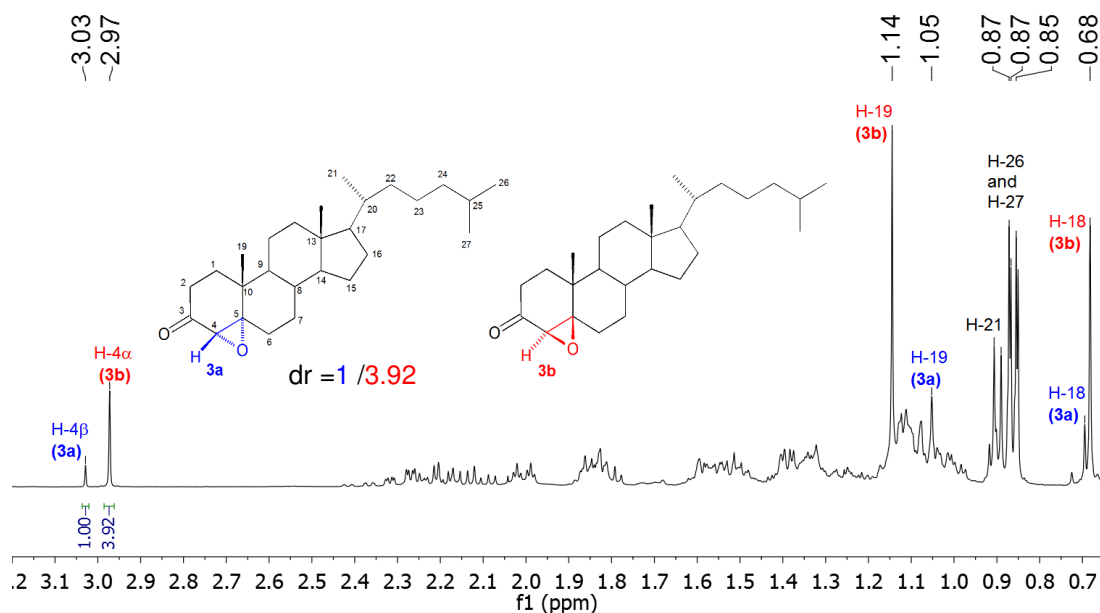


Figure 2. ^1H NMR spectra of the mixtures of the diastereomeric pairs **1a/b**, **2a/b** and **3a/b**.

Table 1. NMR signals of H-4 and H-19 in each pair of epoxides **1a/b**, **2a/b** and **3a/b**

| | α -epoxides | | | β -epoxides | | |
|------|--------------------|-----------|-----------|-------------------|-----------|-----------|
| | 1a | 2a | 3a | 1b | 2b | 3b |
| H-4 | 3.02 | 3.02 | 3.03 | 2.96 | 2.97 | 2.96 |
| H-19 | 1.05 | 1.05 | 1.05 | 1.14 | 1.14 | 1.14 |

^{13}C NMR Analysis

Computational studies

With the crystalline structures of epoxide **1a** and **1b** in hand, the ^{13}C NMR spectra such compounds were simulated in order to assist, confirm or correct the assignments of the NMR signals. Even though the employed computational code allows obtaining absolute chemical shifts, the values are reported as relative to TMS to facilitate comparisons with the experimental data.

Relative chemical shifts (δc) were estimated by using the corresponding tetramethylsilane (TMS) shielding calculated as:

$$\delta\text{c} = \sigma_{\text{TMS}} - \sigma \quad (1)$$

In addition, the δc values were improved by using the procedure suggested by Forsyth and Seabag.¹² It consists on scaling the theoretical shielding values using the slope (a) and intercept (b) obtained from a linear regression analysis of experimental chemical shifts and the calculated

shieldings. It should be noted that the values of parameters a and b are generally method- and basis-set dependent, but the a value is expected to be close to 1. This procedure has been successfully employed,¹³⁻¹⁶ and is currently accepted as a reliable way of improving NMR data obtained from calculations. In the present study the correlation σc vs. δ^{exp} has been used for that purpose, and thus the scaled values correspond to:

$$\delta c^{\text{scal}} = (\sigma c - b)/a \quad (2)$$

The calculated ^{13}C isotropic chemical shielding of TMS was found to be 193.6 ppm, i.e. 5.5 ppm larger than the experimental value is (188.1 ppm).¹⁷ Since it is a significant deviation, to calculate the relative ^{13}C chemical shifts of epoxides **1a** and **1b**, two different approaches were employed. The first one is to use the computed absolute shift of TMS as reference in the calculation of the relative values to obtain δc (Equation 1), and the other one to use the Forsyth and Seabag procedure¹² to obtain scaled values of the chemical shifts (δc^{scal} , Equation 2)

The linear correlations for the latter case are shown in Figure 3. The slope in both cases is ≈ -1 and the correlation coefficients (R^2) values are ≈ 1 , which supports the reliability of the calculated ^{13}C NMR data. In addition, this value simplifies the form of Equation 2, leading to a scaling procedure consisting only on adjustments based on subtraction from a fixed reference. Accordingly, the expressions used to calculate the δc^{scal} values for epoxides **1a** and **1b** are:

$$\delta c^{\text{scal (1a)}} = 189.02 - \sigma c^{(1a)} \quad (3)$$

$$\delta c^{\text{scal (1b)}} = 189.24 - \sigma c^{(1b)} \quad (4)$$

It is interesting to notice that the b values obtained from the correlations are very similar for epoxides **1a** and **1b** (189.02 and 189.24 ppm, respectively), supporting the consistency of the calculations at the given level of theory.

The calculated values are listed in Table 2, together with the deviations from the experimental values and the corresponding mean unsigned errors (MUE). It was found that the non-scaled chemical shifts (δc , Equation 1) lead to Mean Unsigned Errors (MUE) values of 4.3 and 4.2 ppm, for epoxides **1a** and **1b**, respectively. The agreement between the calculated and the experimental data is significantly improved when the scaling procedure is used (δc^{scal} , Equations 3 and 4), leading to MUE values equal to 1.1 ppm for both epoxides **1a** and **1b**. It should be noted, however, that the trend of the calculated signals is the same regardless the procedure used to calculate the chemical shifts.

Table 2. Experimental and calculated ^{13}C NMR signals of epoxides **1a** and **1b** (δc , ppm), deviations with respect to the experimental values ($D\text{v}$, ppm),^(a,b) and Mean Unsigned Errors (MUE, ppm)^(c)

| C# | 1a | | | | | 1b | | | | |
|------------------------------|-----------------------|------------------|-------------------|--------------------------------|------------------------------|-----------------------|------------------|-------------------|--------------------------------|---------------------------|
| | δ^{exp} | δc | $D\text{v}^{(a)}$ | $\delta\text{c}^{\text{scal}}$ | $D\text{v}^{\text{scal}(b)}$ | δ^{exp} | δc | $D\text{v}^{(a)}$ | $\delta\text{c}^{\text{scal}}$ | $D\text{v}^{\text{scal}}$ |
| 1 | 29.0 | 33.4 | 4.4 | 28.8 | -0.2 | 26.1 | 29.9 | 3.8 | 25.6 | -0.5 |
| 2 | 33.0 | 37.3 | 4.3 | 32.7 | -0.3 | 32.4 | 36.8 | 4.4 | 32.4 | 0.0 |
| 3 | 206.6 | 211.3 | 4.7 | 206.7 | 0.1 | 206.4 | 211.8 | 5.4 | 207.4 | 1.0 |
| 4 | 62.7 | 66.5 | 3.8 | 61.9 | -0.8 | 62.5 | 66.3 | 3.8 | 61.9 | -0.6 |
| 5 | 69.9 | 76.0 | 6.1 | 71.4 | 1.5 | 70.0 | 75.1 | 5.1 | 70.8 | 0.8 |
| 6 | 29.5 | 34.0 | 4.5 | 29.4 | -0.1 | 29.7 | 34.1 | 4.4 | 29.7 | 0.0 |
| 7 | 28.4 | 33.4 | 5.0 | 28.9 | 0.5 | 29.8 | 34.3 | 4.5 | 29.9 | 0.1 |
| 8 | 35.2 | 40.5 | 5.3 | 36.0 | 0.8 | 34.8 | 40.1 | 5.3 | 35.8 | 1.0 |
| 9 | 50.6 | 56.4 | 5.8 | 51.8 | 1.2 | 46.4 | 50.9 | 4.5 | 46.5 | 0.1 |
| 10 | 36.7 | 44.0 | 7.3 | 39.4 | 2.7 | 37.2 | 44.3 | 7.1 | 40.0 | 2.8 |
| 11 | 21.1 | 25.9 | 4.8 | 21.4 | 0.3 | 21.1 | 26.0 | 4.9 | 21.7 | 0.6 |
| 12 | 36.6 | 40.8 | 4.2 | 36.3 | -0.3 | 36.4 | 40.7 | 4.3 | 36.4 | 0.0 |
| 13 | 42.5 | 48.3 | 5.8 | 43.7 | 1.2 | 42.6 | 48.4 | 5.8 | 44.1 | 1.5 |
| 14 | 49.9 | 54.7 | 4.8 | 50.1 | 0.2 | 50.2 | 54.7 | 4.5 | 50.3 | 0.1 |
| 15 | 23.4 | 28.0 | 4.6 | 23.4 | 0.0 | 23.4 | 28.1 | 4.7 | 23.8 | 0.4 |
| 16 | 27.4 | 31.6 | 4.2 | 27.0 | -0.4 | 27.4 | 31.9 | 4.5 | 27.5 | 0.1 |
| 17 | 82.4 | 87.8 | 5.4 | 83.2 | 0.8 | 82.4 | 88.1 | 5.7 | 83.8 | 1.4 |
| 18 | 11.9 | 14.1 | 2.2 | 9.6 | -2.3 | 12.0 | 14.3 | 2.3 | 10.0 | -2.0 |
| 19 | 16.5 | 18.3 | 1.8 | 13.8 | -2.7 | 18.9 | 21.0 | 2.1 | 16.7 | -2.2 |
| CH₃ acetyl | 20.8 | 22.5 | 1.7 | 18.0 | -2.8 | 21.0 | 22.4 | 1.4 | 18.0 | -3.0 |
| C=O acetyl | 170.9 | 171.4 | 0.5 | 166.9 | -4.0 | 171.0 | 171.4 | 0.4 | 167.1 | -3.9 |
| MUE^(c) | | | 4.3 | | 1.1 | | | 4.2 | | 1.1 |

Legend: ^(a) $D\text{v} = \delta\text{c} - \delta^{\text{exp}}$

^(b) $D\text{v}^{\text{scal}} = \delta\text{c}^{\text{scal}} - \delta^{\text{exp}}$

^(c) $MUE = \frac{\sum_{i=1}^N |\delta\text{c} - \delta^{\text{exp}}|}{N}$

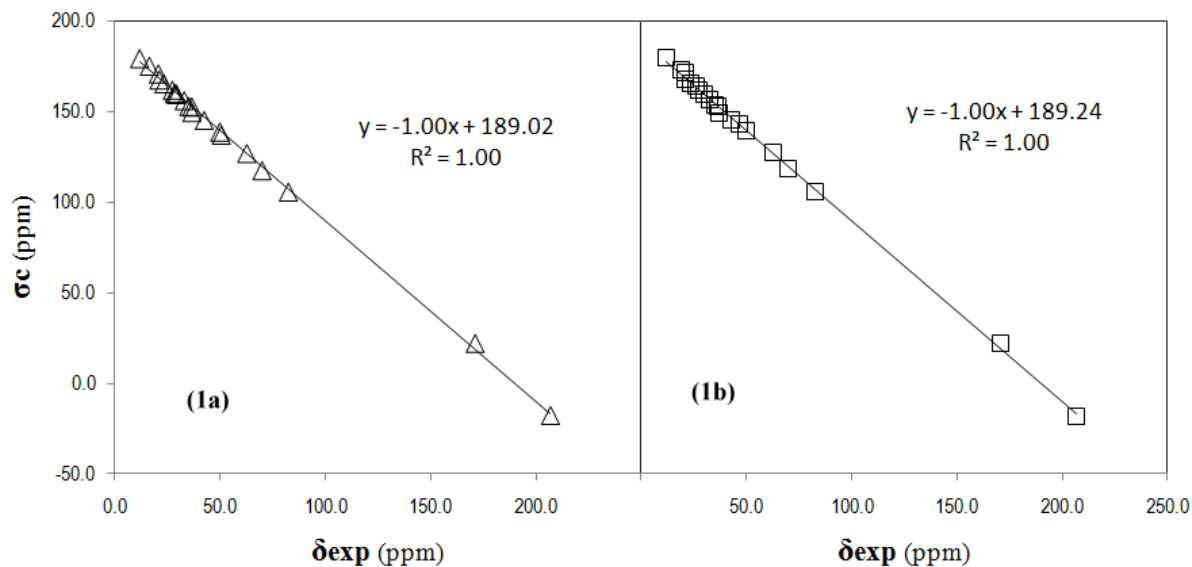


Figure 3. Linear regression analyses of calculated shielding (σ_c) vs experimental chemical shifts (δ_{exp}) for epoxides **1a** and **1b**.

^{13}C NMR signals assignments and shielding effects

The chemical shifts associated to the C/D rings and the side chains of are in good agreement with the previously available shielding data.¹⁸ Assignments of the signals corresponding to the A/B rings in compounds **2a/b** and **3a/b** are in good agreement with the data obtained above for compounds **1a/b** (see Table 3). The fact that, regardless the differences in the side chains, similar shielding profiles are observed amongst the α - or β -epoxides, accounts for the accuracy of both, the theoretical and experimental assignments.

Comparison of the NMR spectra of each α/β pair shows that the resonance signal of C-9 in the β -epoxides is shifted -4.2 ppm respect to that of the α -counterpart. Electronic compression of H-9 α exerted by the C-2 methylene may justify this effect that is only present in the β -epoxides. A similar, but lower (-2.9 ppm) upfield shift is observed in the β -epoxides when their C-1 signals are compared with those of the α -partner and can be interpreted as the result of an O \leftrightarrow H-1 β interaction that in the β -epoxides compress H-1 β and results in the shielding of C-1.

Downfield shifts in the signals of C-7 and C-19 of the β -epoxide are observed when compared to those of the α -partner. In the case of C-19, the observed effect may be interpreted as the result of the absence of the δ -syn H-2 β \leftrightarrow H-19 interaction that in the α -epoxides shields C-19. Downfield shift of the signal of C-7 in the β -epoxides may be considered a consequence of the absence the O \leftrightarrow H-7 α syn interaction that in the α -epoxides shields C-7 (see Table 3 and Figure 4).

Table 3. Assignments of the ^{13}C NMR experimental signals of the studied pairs of diastereomeric epoxides **1a/b**, **2a/b** and **3a/b** (δ ppm)

| C# | δ (1a) | δ (1b) | $\Delta[\delta_{(1b)}-\delta_{(1a)}]$ | δ (2a) | δ (2b) | $\Delta[\delta_{(2b)}-\delta_{(2a)}]$ | δ (3a) | δ (3b) | $\Delta[\delta_{(3b)}-\delta_{(3a)}]$ |
|------------------------------|---------------|---------------|---------------------------------------|---------------|---------------|---------------------------------------|---------------|---------------|---------------------------------------|
| 1 | 29.0 | 26.1 | -2.9 | 29.1 | 26.1 | -3.0 | 29.1 | 26.1 | -3.0 |
| 2 | 33.0 | 32.4 | -0.6 | 33.0 | 32.5 | -0.5 | 33.1 | 32.6 | -0.5 |
| 3 | 206.6 | 206.4 | -0.2 | 206.7 | 206.6 | -0.1 | 207.2 | 206.9 | -0.3 |
| 4 | 62.7 | 62.5 | -0.2 | 62.8 | 62.6 | -0.2 | 62.9 | 62.7 | -0.2 |
| 5 | 69.9 | 70.0 | +0.1 | 70.0 | 70.2 | +0.2 | 70.3 | 70.5 | +0.2 |
| 6 | 29.5 | 29.7 | +0.2 | 29.6 | 29.7 | +0.1 | 29.8 | 29.9 | +0.1 |
| 7 | 28.4 | 29.8 | +1.4 | 28.8 | 30.3 | +1.5 | 29.0 | 30.4 | +1.4 |
| 8 | 35.2 | 34.8 | -0.4 | 35.3 | 35.0 | -0.3 | 35.4 | 35.0 | -0.4 |
| 9 | 50.6 | 46.4 | -4.2 | 50.5 | 46.4 | -4.1 | 50.7 | 46.4 | -4.3 |
| 10 | 36.7 | 37.2 | +0.5 | 36.7 | 37.2 | +0.5 | 36.7 | 37.2 | +0.5 |
| 11 | 21.1 | 21.1 | 0 | 21.4 | 21.5 | +0.1 | 21.4 | 21.5 | +0.1 |
| 12 | 36.6 | 36.4 | -0.2 | 38.7 | 38.4 | -0.3 | 39.7 | 39.4 | -0.3 |
| 13 | 42.5 | 42.6 | +0.1 | 44.0 | 44.1 | +0.1 | 42.5 | 42.6 | +0.1 |
| 14 | 49.9 | 50.2 | +0.3 | 55.8 | 55.9 | +0.1 | 55.6 | 55.8 | +0.2 |
| 15 | 23.4 | 23.4 | 0 | 24.4 | 24.3 | -0.1 | 23.8 | 23.8 | 0 |
| 16 | 27.4 | 27.4 | 0 | 22.8 | 22.8 | 0 | 28.2 | 28.0 | -0.2 |
| 17 | 82.4 | 82.4 | 0 | 63.6 | 63.4 | -0.2 | 56.2 | 56.1 | -0.1 |
| 18 | 11.9 | 12.0 | +0.1 | 13.3 | 13.3 | 0 | 12.0 | 12.0 | 0 |
| 19 | 16.5 | 18.9 | +2.4 | 16.5 | 19.0 | +2.5 | 16.5 | 19.0 | +2.5 |
| 20 | - | - | - | 209.2 | 209.1 | -0.1 | 35.8 | 35.7 | -0.1 |
| 21 | - | - | - | 31.5 | 31.4 | -0.1 | 18.7 | 18.6 | -0.1 |
| 22 | - | - | - | - | - | - | 36.1 | 36.1 | 0 |
| 23 | - | - | - | - | - | - | 24.2 | 24.2 | 0 |
| 24 | - | - | - | - | - | - | 39.5 | 39.5 | 0 |
| 25 | - | - | - | - | - | - | 28.0 | 28.1 | +0.1 |
| 26 | - | - | - | - | - | - | 22.8 | 22.8 | 0 |
| 27 | - | - | - | - | - | - | 22.6 | 22.5 | -0.1 |
| CH₃ acetyl | 20.8 | 21.0 | +0.2 | - | - | - | - | - | - |
| C=O acetyl | 170.9 | 171.0 | +0.1 | - | - | - | - | - | - |

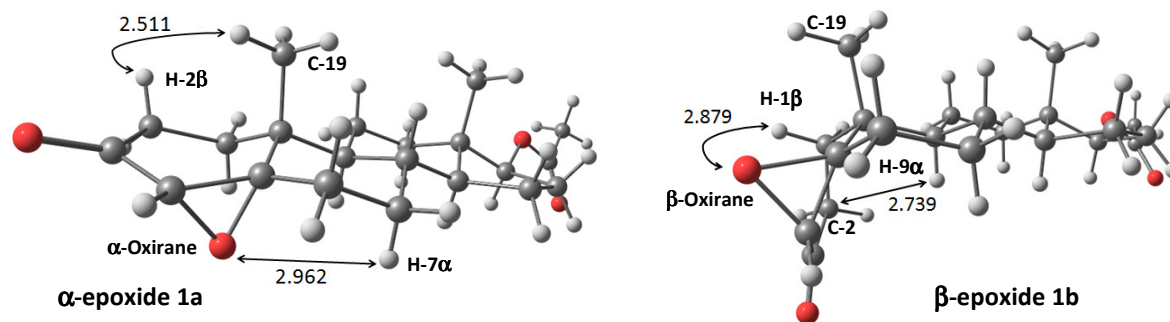


Figure 4. Molecular models of the epoxides **1a** and **1b** generated from the crystal data (distances in Å)

Crystallographic studies

In compound **1a** the A/B, B/C and C/D rings junctions are *trans* and bear β -oriented methyl groups attached to C-10 and C-13. The average magnitude of the C–C distance of the steroid framework in compound **1a** is 1.53 Å, although it should be considered that the bond lengths, C-2–C-3, C-3–C-4 and C-4–C-5, are below the average and below the shortened values found in androsterone.¹⁹ This effect may be attributed not only to the distortion exerted by the epoxy moiety, but also to the effect of the carbonyl group at C-3 that delocalizes π electrons in the nearly planar grouping C-2, C-3, C-4, O-4 [rms deviation of fitted atoms = 0.0126 Å]. Consequently the A ring assumes a distorted half-chair conformation [puckering parameters:²⁰ $Q = 0.4957(2)$ Å, $\theta = 66.84(3)$, $\phi = 335.8(5)^\circ$, if the calculation starts from C-1 to C-10 and proceeds in a counterclockwise direction] with asymmetry parameters²¹ $\Delta C_2(C-2-C-3) = 60.10(5)$, $\Delta C_2(C3-C4) = 7.97(5)$, $\Delta C_2(C4-C5) = 52.20(5)$, $\Delta C_s(C-3) = 32.05(4)$ and $\Delta C_s(C-5) = 52.94(4)^\circ$.

The B ring assumes a chair conformation [puckering parameters $Q = 0.5628(4)$ Å, $\theta = 4.94(4)$, $\phi = 178.78(4)^\circ$, if the calculation starts from C-5 to C-10 and proceeds in a counterclockwise direction]; rotational symmetry is dominant; a pseudo- C_2 axis bisects the C-6–C-7 bond with asymmetry parameters $\Delta C_2(C-6-C-7) = 4.95(4)^\circ$ and $\Delta C_s(C-7) = 2.89(2)^\circ$. The average magnitude of the torsion angles is $55.2(2)^\circ$. Ring C also assumes an almost perfect chair conformation [puckering parameters $Q = 0.5666(5)$ Å, $\theta = 8.50(3)$ and $\phi = 263.07(6)^\circ$ if the calculation starts from C-8 to C-14 and proceeds in a clockwise direction]. The five-membered D ring, which bears the 17β -acetoxy group presents, an envelope conformation on C-13 [puckering parameters $q_2 = 0.4638(4)$ Å and $\phi_2 = 188.90(4)^\circ$] with asymmetry parameters:²² $\Delta = 701.7$, $\tau_m = 47.4(2)$, $\Delta C_s(C13) = 8.99(3)$ and $\Delta C_2(C-13, C-14) = 11.94(3)^\circ$; (see Figure 1).

In the crystal structure of **1a**, each molecule features pairs of C–H \cdots O bonds to its neighbors related by the symmetry operations $-1+x,y,z$ and $2-x,1/2+y,-z$ for C-15–H-15a \cdots O-2 (2.52 Å) and C-18–H-18c \cdots O-3 (2.56 Å) respectively (Figure 5). These intermolecular interactions of type hydrogen bond are observed along the plane formed by the crystallographic *b* and *c* axes, lead to infinite ribbons of $R_2^2(7)$ and *D* motifs.²³

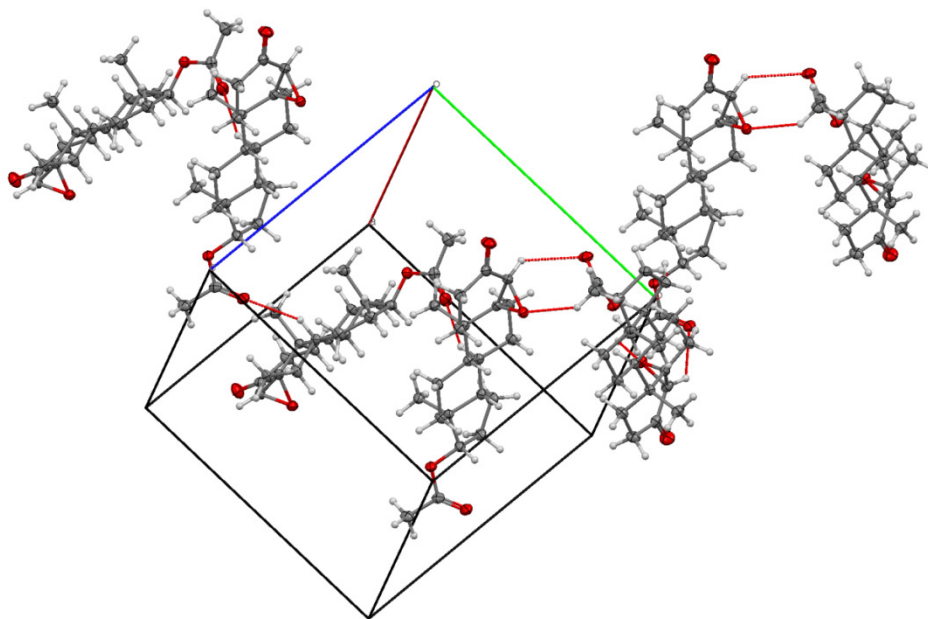


Figure 5. Crystal structure of compound **1a** view along the axis a ; with perspective to plane formed by b and c axes emphasizing the $R^2_2(7)$ and D motifs.

The asymmetric unit of the β -epoxide **1b** consist of two independent units of 17 β -acetoxy-4,5-epoxy-5 β -androstan-3-one, *molecule A* and *molecule B* with *cis A/B*. Compound **1b** has *trans B/C* and *C/D* rings junctions and bears methyl groups attached to C-10 and C-13 in the β -side (see Figure 6). As described for compound **1a**, in both *molecules A* and *B* of the epoxide **1b** the average magnitude of the C-2–C-3, C-3–C-4 and C-4–C-5 distances are rather below the 1.53 Å average and below the shortened values found in androsterone.¹⁹

Table 4. Least-square overlay analysis for each pair of *molecules A* and *B* of compound **1b**

| Rings | <i>Molecule-A</i> vs <i>Molecule-B</i> |
|-------|--|
| A | 0.0672 |
| B | 0.0194 |
| C | 0.0163 |
| D | 0.0101 |

In *molecule B* the O-3 of the 17 β -acetoxy shows disorder in two positions (O-3b and O-3p) with 70:30 of O-3b:O-3p occupancy respectively. In order to establish differences among the studied *molecules A* and *B* of compound **1b**, a least-squares overlay analysis of the structures by pairs was performed. Table 4 shows the results obtained with the Mercury program.²⁴ Small differences are observed in the A ring (rms 0.0672) and in the torsion angles of 170.64 and

177.58° of the 17 β -acetoxy group respectively bonded to C-17a and C-17b (notice that the observed deviations in rings A to D are less than 0.0673).

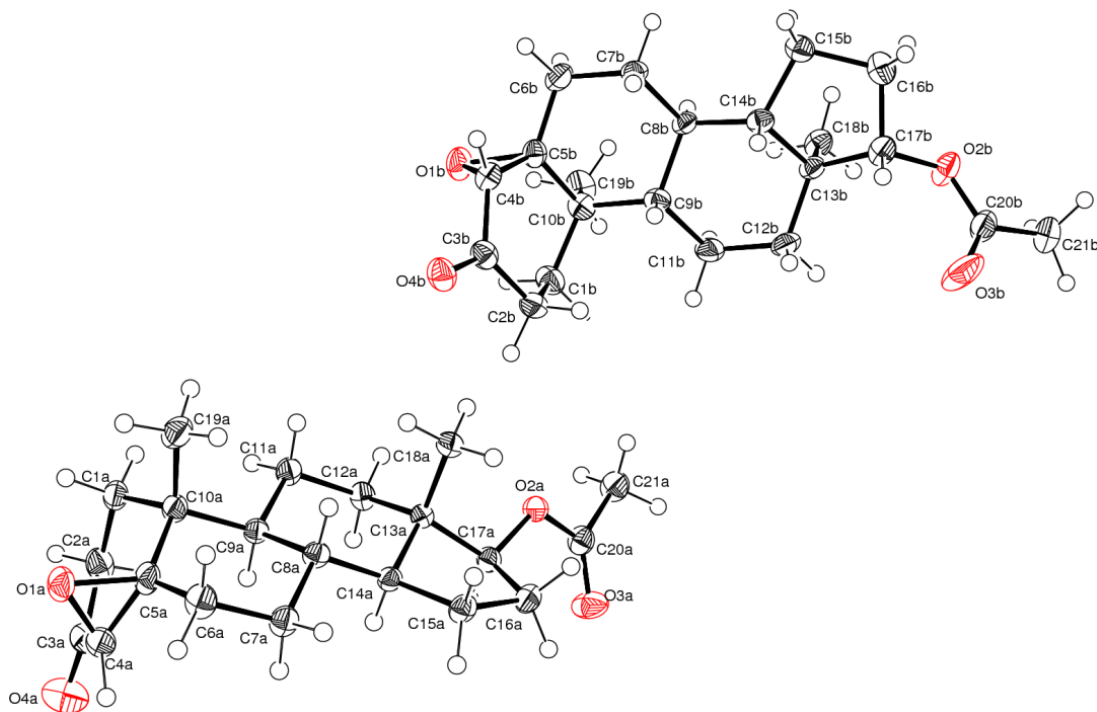


Figure 6. ORTEP drawing of the asymmetric unit of epoxide **1b** showing *molecules A and B* with the thermal ellipsoids drawn at the 50% of probability.

The main bonds contacts present in compound **1b** are intermolecular hydrogen bonds C—H \cdots O. Only *molecule B* shows one intramolecular contact between the C-17b donor atom and O-3b acceptor atom (2.35 Å). Each *molecule A and B* show C—H \cdots O bonds with its neighbors related by the symmetry operation $1-x, -1/2+y, -z$. All these complex interactions form a crystal array with pairs of molecules forming layers parallel to plane c-b (see Figure 7).

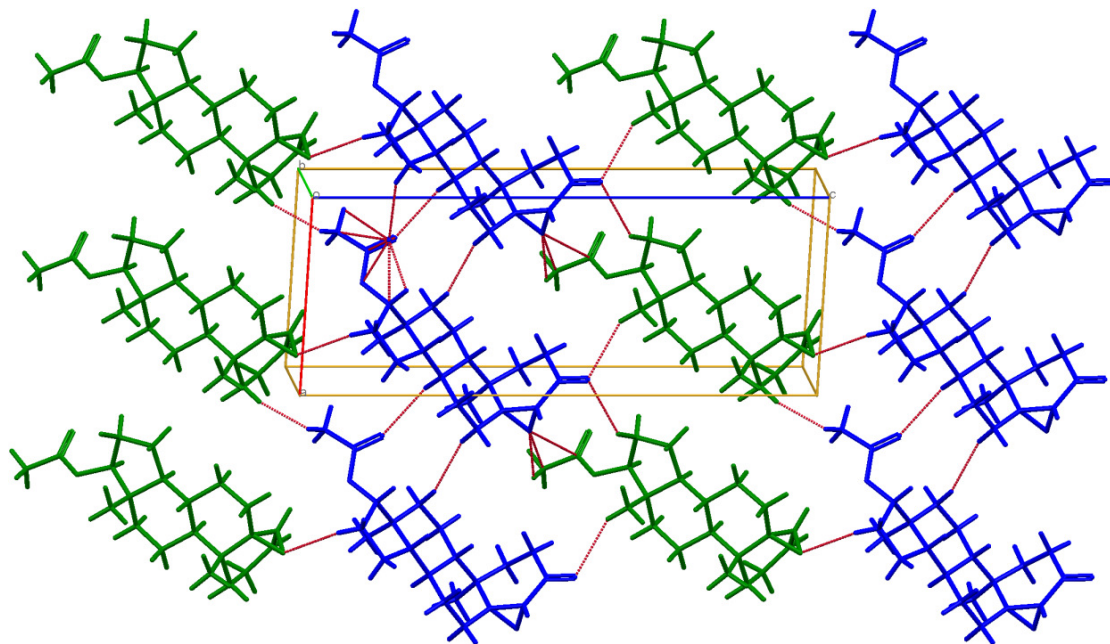


Figure 7. Crystal structure of epoxide **1b** viewed along the *b* axis, showing the short contacts between the symmetry equivalent for *molecule A* (green) and *molecule B* (blue) extending along the *c-b* plane.

Conclusion

The generalized practice for the determination of orientation of substituents in the steroid framework by observation of NOE effects, fails in the case of 4,5-epoxy-3-oxo steroids. After the unambiguous identification of the α - and β -diastereomers by X-ray studies, a fast and reliable criteria, based on the chemical shifts of H-4 and H-19 of each diastereomer, allows both the identification and quantification of each component in the crude reaction mixtures.

Complete and unambiguous assignments of the ^{13}C signals of the studied compounds based on a combination of 1D and 2D NMR techniques was assisted by calculation of absolute isotropic ^{13}C NMR shieldings using the Gauge. The agreement between the experimental assignment and theoretical results accounts for the accuracy of both, the experimental and theoretical data.

Experimental Section

Synthesis and NMR

Reactions were monitored by TLC on ALUGRAM® SIL G/UV254 plates from MACHEREY-NAGEL. Chromatographic plates were sprayed with a 1% solution of vanillin in 50% HClO_4 and heated until color developed. Melting points were measured on a Melt-Temp II equipment and are uncorrected. Mass spectra were registered in a Thermo-Electron spectrometer model DFS

(Double Focus Sector). NMR spectra were recorded in CDCl₃ solution in a Varian INOVA 400 spectrometer using the solvent signal 7.26 ppm for ¹H and 77.00 ppm for ¹³C as references. ¹³C NMR signals assignments in each epoxide were made with the aid of a combination of 2D homonuclear (¹H-¹H) and heteronuclear (¹H-¹³C) correlation techniques, which included Correlation Spectroscopy (COSY), Nuclear Overhauser Effect Spectroscopy (NOESY), Heteronuclear Single Quantum Correlation (HSQC) and Heteronuclear Multiple Bond Correlation (HMBC). All 2D NMR spectra were recorded using the standard pulse sequences and parameters recommended by the manufacturer and processed employing the NMR processing program MestreNova [See <http://mestrelab.com/>].

General epoxidation procedure. NaOH 6N (2 mL) and H₂O₂ 30% (3.1 ml) were added to a solution of the 4-en-3-oxo-steroid (2 mmol) and the mixture was stirred for 90 min before pouring into ice-water (300 mL) and extraction with ethyl acetate (2x125 mL). The organic layer was washed with water to achieve neutrality (12x50 mL), dried (anh. Na₂SO₄) and evaporated to afford a mixture of the corresponding epimeric 4,5-epoxy-3-oxo-steroids.

Reacetylation procedure for the mixture of 1a/1b. The crude mixture resulting from the epoxidation of testosterone acetate (**1**) was dissolved in pyridine (5 ml). Acetic anhydride (1 mL) and a few crystals of DMAP were added and the mixture was stirred for 24 h, poured into ice-H₂O (200 mL) and extracted with ethyl acetate (4 x 50 mL). The organic layer was washed with H₂O (8x40 mL), 10% aqueous CuSO₄ solution, water (8x40 mL), dried (anh. Na₂SO₄) and evaporated to afford 487.3 mg (70.3 % overall yield for the epoxidation-reacetylation sequence) of the 1/3.30 mixture of the epimeric epoxides **1a** and **1b**. Exhaustive chromatographic separation afforded analytical samples of each epoxide.

17β-Acetoxy-4,5-epoxy-5α-androstan-3-one (1a). Mp 160-162 °C (from ethyl acetate) ¹H NMR (CDCl₃, 400 MHz) δ 4.60 (dd, *J* 9.2, 7.8 Hz, 1H, H-17α), 3.02 (s, 1H, H-4β), 2.38 (1H, ddd, *J* 19.9, 7.4, 1.7 Hz H-2α), 2.24 (1H, dd, *J* 19.6, 7.7 Hz, H-2β), 2.01 (s, 3H, CH₃ acetyl), 1.05 (d, *J* 0.8 Hz, 3H, H-19), 0.81 (s, 3H, H-18). For ¹³C NMR (CDCl₃, 100 MHz) see Table 3. MS (EI, 70 eV) 347 (MH⁺, 4%), 346 (M⁺, 13%), 328 (M⁺- H₂O, 12), 319 (10), 318 (M⁺- C=O, 50), 304 (25), 303 (36), 287 (11), 286 (M⁺- CH₃COOH, 42), 274 (74), 273 (13), 272 (15), 271 (28), 268 (16), 258 (15), 257 (28), 240 (16), 239 (25), 231 (24), 229 (10), 225 (11), 215 (36), 213 (77), 212 (18), 211 (11), 202 (11), 201 (49), 200 (18), 199 (60), 197 (19), 189 (12), 187 (25), 186 (16), 185 (26), 183 (12), 175 (18), 174 (19), 173 (62), 172 (17), 171 (33), 165 (11), 163 (14), 161 (28), 160 (21), 159 (49), 158 (14), 157 (26), 151 (11), 149 (29), 148 (33), 147 (100), 146 (41), 45 (70), 144 (21), 143 (24), 138 (10), 137 (14), 136 (12), 135 (36), 134 (26), 133 (63), 132 (18), 131 (50), 129 (13), 125 (17), 124 (10), 123 (38), 122 (14), 121 (50), 120 (26), 119 (61), 118 (12), 117 (20), 113 (11), 111 (16), 110 (21), 109 (38), 108 (17), 107 (66), 106 (19), 105 (80), 97 (27), 96 (13), 95 (57), 94 (25), 93 (89), 92 (13), 91 (70), 83 (14), 81 (78), 80 (13), 79 (72), 77 (37), 68 (10), 67 (57), 65 (12), 57 (14), 55 (68), 53 (25). HRMS (EI, 70 eV) observed 346.2132 required for C₂₁H₃₀O₄ 346.2139.

17 β -Acetoxy-4,5-epoxy-5 β -androstan-3-one (1b). Mp 140-142 °C (*from ethyl acetate*) ^1H NMR (CDCl_3 , 400 MHz) δ 4.57 (ddd, J 9.2, 7.7, 1.2 Hz, 1H, H-17 α), 2.96 (d, J 1.4 Hz, 1H, H-4 α), 2.28 (H-2 α), 2.12 (H-2 β), 2.02 (s, 3H, CH_3 acetyl), 1.14 (s, 3H, H-19), 0.80 (s, 3H, H-18). For ^{13}C NMR (CDCl_3 , 100 MHz) see Table 3. MS (EI, 70 eV) 347 (MH^+ , 3%), 346 (M^+ , 10%), 318 (M^+ - C=O, 37) 304 (25), 303 (55), 286 (M^+ - CH_3COOH , 35), 275 (20), 274 (56), 273 (11), 272 (13), 271 (22), 268 (15), 258 (18), 257 (25), 243 (11), 240 (22), 239 (27), 232 (11), 231 (34), 230 (15), 229 (11), 225 (14), 215 (38), 214 (100), 213 (88), 212 (21), 211 (12), 203 (13), 202 (10), 201 (44), 200 (18), 199 (58), 197 (19), 191 (12), 189 (12), 187 (28), 186 (15), 185 (27), 183 (14), 175 (19), 174 (19), 173 (69), 172 (16), 171 (35), 163 (13), 161 (27), 159 (50), 158 (14), 157 (31), 148 (35), 147 (93), 146 (33), 145 (67), 144 (19), 143 (26), 137 (14), 136 (11), 135 (33), 134 (23), 133 (60), 132 (16), 131 (50), 129 (14), 125 (19), 124 (11), 123 (39), 122 (16), 121 (46), 120 (23), 119 (62), 118 (11), 117 (22), 113 (10), 111 (17), 110 (25), 109 (40), 108 (17), 107 (63), 106 (19), 105 (81), 97 (26), 95 (56), 94 (25), 93 (91), 92 (13), 91 (77), 83 (15), 82 (11), 81 (76), 80 (13), 79 (75), 77 (35), 69 (20), 68 (10), 67 (57), 65 (10), 55 (66), 53 (20). HRMS (EI, 70 eV) observed 346.2127 required for $\text{C}_{21}\text{H}_{30}\text{O}_4$ 346.2139.

The general epoxidation procedure when applied to 2 mmol of progesterone (**2**) afforded 405 mg (61.3 %) of a 1/1.81 mixture of the epoxides **2a/2b**.

4,5-Epoxy-5 α -pregnan-3,20-dione (2a). Colorless oil as a mixture with **2b**. ^1H NMR (400 MHz, CDCl_3) δ 3.02 (s, 1H, H-4 β), 2.39 (H-2 α), 2.20 (H-2 β), 2.11 (s, 3H, H-21), 1.05 (s, 3H, H-19), 0.64 (s, 3H, H-18). For ^{13}C NMR (CDCl_3 , 100 MHz) see Table 3.

4,5-Epoxy-5 β -pregnan-3,20-dione (2b). Colorless oil as a mixture with **2a**. ^1H NMR (400 MHz, CDCl_3) δ 2.97 (s, 1H, H-4 α), 2.27 (H-2 α), 2.15 (H-2 β), 2.10 (s, 3H, H-21), 1.14 (s, 3H, H-19), 0.63 (s, 3H, H-18). For ^{13}C NMR (CDCl_3 , 100 MHz) see Table 3.

The general epoxidation procedure when applied to 2 mmol of cholest-4-en-3-one (**3**) afforded 733 mg (86.7 %) of a 1/3.92 mixture of the epoxides **3a/3b**. Exhaustive chromatographic separation afforded analytical samples of each epoxide.

4,5-Epoxy-5 α -cholestan-3-one (3a). Mp 118 °C (*from hexane-acetone*) Lit.⁴ 123-124 °C. ^1H NMR (400 MHz, CDCl_3) δ 3.03 (s, 1H, H-4 β), 2.39 (ddd, J 19.7, 7.2, 1.2 Hz, 1H, H-2 α), 2.24 (dd, J 19.8, 7.2 Hz, 1H, H-2 β), 1.05 (s, 3H H-19), 0.91 (d, J = 6.5 Hz, 3H, H-21), 0.87 (d, J = 6.6 Hz, 3H, H-26), 0.86 (d, J = 6.6 Hz, 3H, H-27), 0.69 (s, 3H, H-18). For ^{13}C NMR (CDCl_3 , 100 MHz) see Table 3.

4,5-Epoxy-5 β -cholestan-3-one (3b). Mp 118-119 °C (*from hexane-acetone*) Lit.⁴ 118-119. ^1H NMR (400 MHz, CDCl_3) δ 2.96 (s, 1H, H-4 α), 2.28 (ddd, J 19.4, 5.9, 2.2 Hz, 1H, H-2 α), 2.11 (dd, J 19.4, 6.6 Hz, 1H, H-2 β), 1.14 (s, 3H, H-19), 0.89 (d, J = 6.5 Hz, 3H, H-21), 0.86 (d, J = 6.6 Hz, 3H, H-26), 0.85 (d, J = 6.6 Hz, 3H, H-27), 0.68 (s, 3H, H-18). For ^{13}C NMR (CDCl_3 , 100 MHz) see Table 3.

X-ray crystal structure determination

Suitable crystals for X-Ray diffraction studies were obtained by slow evaporation of the ethyl acetate solutions of epoxides **1a** and **1b** at room temperature. Crystals of compounds **1a** and **1b**

mounted on glass fiber were studied with Oxford Diffraction Gemini "A" diffractometer with a CCD area detector ($\lambda_{\text{MoK}\alpha} = 0.71073 \text{ \AA}$, monochromator: graphite) source equipped with a sealed tube X-ray source at 130 K. Unit cell constants were determined with a set of 15/3 narrow frame/runs (1° in ω) scans. A data sets consisted of 133 and 183 frames of intensity data collected for the epoxides **1a** and **1b** respectively with a frame width of 1° in ω , a counting time of 10 s/frame, and a crystal-to-detector distance of 55.00 mm. The double pass method of scanning was employed to exclude any noise. The collected frames were integrated by using an orientation matrix determined from the narrow frame scans.

Crystallographic data have been deposited with the Cambridge Crystallographic Data Center as supplementary material numbers CCDC 899268 (compound **1a**) and CCDC 899269 (compound **1b**). Copies of the data can be obtained free of charge on application to CCDC, 12 Union Road, Cambridge CB2 1EZ, UK. fax: +44(0)1223-336033; email: deposit@ccdc.cam.ac.uk, or from www.ccdc.cam.ac.uk/conts/retrieving.html.

Table 5. Crystal data and structure refinement parameters for epoxides **1a** and **1b**

| Parameter | 1a | 1b |
|---------------------------------|--|--|
| Empirical formula | C ₂₁ H ₃₀ O ₄ | C ₂₁ H ₃₀ O ₄ |
| Formula weight | 346.45 | 346.45 |
| Temperature | 130(2) K | 130(2) K |
| Wavelength | 0.71073 Å | 0.71073 Å |
| Crystal system | Othorhombic | Monoclinic |
| Space group | P 21 21 21 | P 21 |
| Unit cell dimensions | a = 11.0027(5) Å b = 12.4699(6) Å c = 13.3482(7) Å | a = 8.0076(4) Å b = 11.0905(5) Å c = 20.8099(10) Å β = 93.367(5)° |
| Volume | 1831.41(15) Å ³ | 1844.90(15) Å ³ |
| Z | 4 | 4 |
| Density (calculated) | 1.257 Mg/m ³ | 1.247 Mg/m ³ |
| Absorption coefficient | 0.085 mm ⁻¹ | 0.085 mm ⁻¹ |
| F(000) | 752 | 752 |
| Crystal size | 0.5838 x 0.5547 x 0.5178 mm ³ | 0.5078 0.4554 0.1292mm ³ |
| Theta range for data collection | 3.61 to 26.05°. | 3.47 to 26.04°. |
| Index ranges | -13 ≤ h ≤ 9, -15 ≤ k ≤ 11, -15 ≤ l ≤ 16 | -7 ≤ h ≤ 9, -10 ≤ k ≤ 13, -25 ≤ l ≤ 19 |
| Reflections collected | 5700 | 8127 |
| Independent reflections | 3183 [R(int) = 0.0185] | 5532 [R(int) = 0.0331] |
| Completeness to theta = 26.3° | 99.6 % | 99.7 % |

Table 5. Continued

| Parameter | 1a | 1b |
|--------------------------------------|------------------------------------|------------------------------------|
| Refinement method | Full-matrix least-squares on F2 | Full-matrix least-squares on F2 |
| Data / restraints / parameters | 3183 / 0 / 229 | 5532 / 7 / 461 |
| Goodness-of-fit on F2 | 1.037 | 1.056 |
| Final R indices [$I > 2\sigma(I)$] | R1 = 0.0342, wR2 = 0.0781 | R1 = 0.0440, wR2 = 0.1132 |
| R indices (all data) | R1 = 0.0402, wR2 = 0.0819 | R1 = 0.0514, wR2 = 0.1215 |
| Absolute structure parameter | -0.1(10) | -0.2(10) |
| Largest diff. peak and hole | 0.151 and -0.196 e.Å ⁻³ | 0.173 and -0.208 e.Å ⁻³ |

CrysAlisPro and CrysAlis RED software packages²⁵ were employed for collection and integration of data. Analysis of the integrated data did not reveal any decay. Final cell constants were determined by a global refinement of 5818 and 8298 reflections ($\theta < 26.3^\circ$) for **1a** and **1b** respectively. Collected data were corrected for absorbance by using analytical numeric absorption correction²⁶ using a multifaceted crystal model based on expressions upon the Laue symmetry employing equivalent reflections. Structure solution and refinement were carried out with the programs SHELXS97 and SHELXL97.²⁷ Molecular graphics were generated with ORTEP-3 for Windows and software employed for preparation of the material for publication was WinGX.²⁸

Full-matrix least-squares refinement was carried out by minimizing $(F_o^2 - F_c^2)^2$. All non-hydrogen atoms were refined anisotropically. Hydrogens attached to carbon atoms were placed in geometrically idealized positions and refined employing the riding model, with C–H distances = 0.98 – 1.00 Å with $U_{iso}(\text{H}) = 1.2U_{eq}(\text{C})$ for methylene and methyne groups, and $U_{iso}(\text{H}) = 1.5U_{eq}(\text{C})$ for methyl group. Crystal data and experimental details of the structure refinement are summarized in Table 7.

Computational details. Geometry optimizations and frequency calculations were performed using the B3LYP functional and the 6-31+G(d,p) basis set. They were carried out in solution, using the SMD continuum model²⁹ and chloroform as solvent. Geometries were fully optimized without imposing any restriction, using the X-ray structures as starting points. Local minima were confirmed by the absence of imaginary frequencies. All the electronic calculations were performed with Gaussian 09 package of programs.³⁰ After optimization, the absolute isotropic ¹³C NMR shieldings (σ_c) were calculated using the GIAO (Gauge Invariant Atomic Orbitals) method^{31,32} in chloroform also at B3LYP/6-31+G(d,p) level.

Acknowledgments

The authors thank to *Dirección General de Asuntos del Personal Académico* (DGAPA-UNAM) for financial support via Project IN221911-3 and *Laboratorio de Visualización y Cómputo*

Paralelo at UAM-Iztapalapa for the access to its computer facilities. Thanks are due to Dr. Nuria Esturau Escofet and M.Sc.Georgina Duarte Lisci (USAI-UNAM) for registering NMR and MS spectra. We want to express our gratitude to Dr. Carlos Cobas from Mestrelab® for assistance with the MestreNova NMR processing program.

References

1. Uyanic, C.; Malay, A.; Ayna, A. S.; Hanson, J. R.; Hitchcock, P. B. *Steroids* **2005**, *70*, 71.
<http://dx.doi.org/10.1016/j.steroids.2004.09.002>
PMid:15631862
2. Back, T. G.; Chau, J. H-L.; Coddling, O. W.; Gladstone, P. L.; Jones, D. H.; Morzycki, J. W.; Roszak, A. W. *J. Org. Chem.* **1992**, *57*, 4110.
<http://dx.doi.org/10.1021/jo00041a013>
3. Neeman, M.; O'Grodnick, J.S. *Tetrahedron Lett.* **1972**, *13*, 783.
[http://dx.doi.org/10.1016/S0040-4039\(01\)84438-5](http://dx.doi.org/10.1016/S0040-4039(01)84438-5)
4. Nickon, A.; Mendelson, W. L. *J. Am. Chem. Soc.* **1965**, *87*, 3921–3928.
<http://dx.doi.org/10.1021/ja01095a023>
5. Jennings, B. R.; Bengtson, J. M. *Steroids* **1978**, *31*, 49–67.
[http://dx.doi.org/10.1016/0039-128X\(78\)90019-3](http://dx.doi.org/10.1016/0039-128X(78)90019-3)
6. Bovicelli, P.; Lupattelli, P.; Mincione, E. *J. Org. Chem.* **1992**, *57*, 2182–2184.
<http://dx.doi.org/10.1021/jo00033a053>
7. Carvalho, J. F. S.; Cruz Silva, M. M.; Sá e Melo, M. L. *Tetrahedron* **2009**, *65*, 2773.
<http://dx.doi.org/10.1016/j.tet.2009.01.100>
8. Romero-Ávila, M.; de Dios-Bravo, G.; Méndez-Stivalet, J. M.; Rodríguez-Sotres, R.; Iglesias-Arteaga, M. A. *Steroids* **2007**, *72*, 955.
<http://dx.doi.org/10.1016/j.steroids.2007.08.007>
PMid:17905389
9. Rosado-Abón, A.; Romero-Avila, M.; Iglesias-Arteaga, M. A. *Arkivoc* **2010**, (x), 110.
<http://dx.doi.org/10.3998/ark.5550190.0011.a10>
10. Rosado-Abón, A.; de Dios-Bravo, G.; Rodríguez-Sotres, R.; Iglesias-Arteaga, M. A. *Steroids* **2012**, *77*, 461.
<http://dx.doi.org/10.1016/j.steroids.2012.01.004>
PMid:22273808
11. Rosado-Abón, A.; de Dios-Bravo, G.; Rodríguez-Sotres, R.; Iglesias-Arteaga, M. A. *J. Steroid. Biochem. & Mol. Biol.* **2013**, *134*, 45.
12. Forsyth, D. A.; Seabag, A. B. *J. Am. Chem. Soc.* **1997**, *119*, 9483.
<http://dx.doi.org/10.1021/ja970112z>
13. Barone, G.; Gomez-Paloma, L.; Duca, D.; Silvestri, A.; Riccio, R.; Bifulco, G. *Chem. Eur. J.* **2002**, *8*, 3233.
[http://dx.doi.org/10.1002/1521-3765\(20020715\)8:14<3233::AID-CHEM3233>3.0.CO;2-0](http://dx.doi.org/10.1002/1521-3765(20020715)8:14<3233::AID-CHEM3233>3.0.CO;2-0)

14. Barone, G.; Duca, D.; Silvestri, A.; Gomez-Paloma, L.; Riccio, R.; Bifulco, G. *Chem. Eur. J.* **2002**, *8*, 3240.
[http://dx.doi.org/10.1002/1521-3765\(20020715\)8:14<3240::AID-CHEM3240>3.0.CO;2-G](http://dx.doi.org/10.1002/1521-3765(20020715)8:14<3240::AID-CHEM3240>3.0.CO;2-G)
15. Cheng F, Sun H, Zhang Y, Mukkamala D, Oldfield E *J. Am. Chem. Soc.* **2005**, *127*, 12544.
<http://dx.doi.org/10.1021/ja051528c>
PMid:16144402
16. Mukkamala D.; Zhang Y.; Oldfield E. *J. Am. Chem. Soc.* **2007**, *129*, 7385.
<http://dx.doi.org/10.1021/ja071227y>
PMid:17506558
17. Cheeseman, J. R.; Trucks, G. W.; Keith, T. A.; Frisch, M. J. *J. Chem. Phys.* **1996**, *104*, 5497.
18. Blunt, J. W.; Stothers, J. B. *Org. Magn. Resonance* **1977**, *9*, 439.
<http://dx.doi.org/10.1002/mrc.1270090802>
19. High, D.F.; Kraut, J. *Acta. Crystallogr.* **1966**, *21*, 88-96.
<http://dx.doi.org/10.1107/S0365110X66002378>
PMid:5952605
20. Cremer, D.; Pople, J. A. *J. Am. Chem. Soc.* **1975**, *97*, 1354.
<http://dx.doi.org/10.1021/ja00839a011>
21. Duax, W. L.; Weeks, C. M.; Rohrer, D. C. *Topics in Stereochemistry* Eliel, E. L.; Allinger, N. New York: John Wiley, 1976; Vol. 2, p 271.
<http://dx.doi.org/10.1002/9780470147184.ch5>
22. Altona, C.; Geise, H. J.; Romers, C. *Tetrahedron* **1968**, *24*, 132.
23. Etter, M. C. *Acc. Chem. Res.* **1990**, *23*, 120.
<http://dx.doi.org/10.1021/ar00172a005>
24. Macrae, C. F.; Edgington, P. R.; McCabe, P.; Pidcock, E.; Shields, G. P.; Taylor, R.; Towler, M.; van De Streek, J. *J. Appl. Cryst.* **2006**, *39*, 453.
<http://dx.doi.org/10.1107/S002188980600731X>
25. CrysAlis CCD and CrysAlis R. 2009 Oxford Diffraction, Abingdon.
26. Clark, R. C.; Reid, J. S. *Acta Crystallogr.* **1995**, *A51*, 887.
27. Sheldrick, G. M. *Acta Crystallogr.* **2008**, *A64*, 112.
28. Farrugia, L. J. *J. Appl. Crystallogr.* **2012**, *45*, 849.
<http://dx.doi.org/10.1107/S0021889812029111>
29. Marenich, A. V.; Cramer, C. J.; Truhlar, D. G. *J. Phys. Chem. B.* **2009**, *113*, 6378.
<http://dx.doi.org/10.1021/jp810292n>
PMid:19366259
30. Gaussian 09, Revision A.08, Frisch, M. J.; Trucks, G. W.; Schlegel, H. B.; Scuseria, G. E.; Robb, M. A.; Cheeseman, J. R.; Scalmani, G.; Barone, V.; Mennucci, B.; Petersson, G. A.; et al. Gaussian, Inc., Wallingford CT, 2009.
31. Wolinski, K.; Hilton, J. F.; Pulay, P. *J. Am. Chem. Soc.* **1990**, *112*, 8251.
<http://dx.doi.org/10.1021/ja00179a005>
32. Cheeseman, J. R.; Trucks, G. W.; Keith, T. A.; Frisch, M. J. *J. Chem. Phys.* **1996**, *104*, 5497.